

Sequence Distribution and Stereoregularity of Methyl Methacrylate and Butyl Acrylate Statistical Copolymers Synthesized by Atom Transfer Radical Polymerization

José Luis de la Fuente, Marta Fernández-García, Marina Fernández-Sanz, and Enrique López Madruga*

Instituto de Ciencia y Tecnología de Polímeros (CSIC), Juan de la Cierva 3, 28006 Madrid, Spain

Received March 12, 2001

ABSTRACT: ^1H and ^{13}C NMR spectra of copolymers of methyl methacrylate (M) and butyl acrylate (B) were analyzed in terms of sequence distribution and stereoregularity of monomer units. The copolymers were prepared by atom transfer radical polymerization (ATRP) in bulk and 25% (v/v) benzonitrile solution. The different experimental conditions resulted in different levels of polymerization control. Under our experimental conditions, the experimental data agreed well with data calculated from the Mayo–Lewis terminal model and Bernoullian statistics with monomer reactivity ratios of $r_{\text{M}} = 1.44 \pm 0.11$ and $r_{\text{B}} = 0.56 \pm 0.06$ and an isotacticity parameter of $\sigma_{\text{M}} = 0.23$ and coisotacticity parameter of $\sigma = 0.30$. Therefore, the copolymer compositions and microstructures are independent of the controllability of the ATRP process.

Introduction

The distribution of monomer sequences along the macromolecular chains and their stereochemical configuration significantly influence the polymers' physical–chemical properties and industrial applications. Knowledge of the copolymer microstructure also provides information on the reaction mechanisms that occur during the polymerization.¹ High-resolution nuclear magnetic resonance (NMR) spectroscopy is particularly effective for determining the copolymer microstructure, especially sequence distribution and tacticity.²

Recently, the concept of “living” free-radical polymerization,³ especially atom transfer radical polymerization (ATRP),⁴ has attracted considerable interest due to the advantages of free-radical procedures (reaction conditions are not especially severe) and living procedures (control over molecular weight, chain ends, and macromolecular architecture). Several research groups have carried out living/controlled free radical copolymerizations^{5–9} of methyl methacrylate (M) with butyl acrylate (B); however, to date, there have been no reports on the stereochemical arrangement of monomers in the copolymer chain.

Copolymers synthesized by conventional radical polymerizations show a composition drift between different chains because of the monomers' different reactivity ratios, while copolymers synthesized by controlled radical polymerization only have a drift in composition within the chain. These differences between conventional and controlled copolymerizations may affect the copolymer microstructure. Therefore, to get insight into the methyl methacrylate–butyl acrylate statistical copolymerization, two different series of copolymerization reactions have been made. These two copolymerizations presented very different degrees of control on the molecular weight and molecular weight distribution. The first one was prepared using methyl 2-chloropropionate as initiator and copper chloride/2,2'-bipyridine as catalyst in bulk at 100 °C; the second one was performed using methyl 2-bromopropionate with the same catalyst system (exchange halide) in 25% (v/v) benzonitrile solution at 100 °C. The microstructure and

stereochemical configuration of monomer sequences in the copolymer chains were determined throughout the entire conversion range to confirm the proposed copolymerization model.

Experimental Section

Materials. Methyl methacrylate (>99%, Merck) and butyl acrylate (>99%, Merck) were passed through an alumina column and distilled prior to use. Methyl 2-chloropropionate, MeClPr (99%, Aldrich), methyl 2-bromopropionate, MeBrPr, ($\geq 99\%$, Aldrich), copper chloride, CuCl (99.99%, Aldrich), 2,2'-bipyridine, Bpy ($\geq 99\%$, Aldrich), and benzonitrile (anhydrous 99%, Aldrich) were used as received.

Polymerizations. Random methyl methacrylate–butyl acrylate (M–B) copolymerization at three different feed monomer compositions 75:25, 50:50, and 25:75 were carried out under ATRP conditions using methyl 2-chloropropionate or methyl 2-bromopropionate as initiator, 1 mol equiv of copper chloride as catalyst, and 3 mol equiv of 2,2'-bipyridine as ligand, both relative to initiator, in bulk or benzonitrile 25% (v/v) at 100 °C ([Mon]:[MeXPr]:[CuCl]:[Bpy] = 100:1:1:3). In a typical procedure, the reaction mixtures were introduced into glass ampules, degassed by three cycles of freeze–pump–thaw, and then were sealed under high vacuum. The ampules were placed in an oil bath with preset temperature of 100 ± 0.1 °C. Resulting polymers were isolated as follows: the polymer was dissolved in chloroform and passed through a neutral alumina column to remove catalyst. The most chloroform was removed by rotatory evaporation, and the polymer dissolved in a minimum amount of chloroform was poured into a large excess of hexane for methyl methacrylate or methanol for butyl acrylate and copolymers. The precipitated products were filtered and dried in a vacuum oven at room temperature until a constant weight was reached. Total monomer conversions were measured gravimetrically. Examples of copolymerization are given hereinafter. Bulk copolymerization: 0.867 mmol of methyl 2-chloropropionate, 0.867 mmol of CuCl, and 2.601 mmol of Bpy were mixed with 65.0 mmol of M and 21.7 mmol of B. For a reaction time of 6600 s, the total monomer conversion was 21.7%. Copolymer characterization: butyl acrylate copolymer composition was 0.200, number-average molecular weight determined by gel permeation chromatography was 46 000, and molecular weight distribution was 1.42. Benzonitrile copolymerization: 0.693 mmol of methyl 2-bromopropionate, 0.693 mmol of CuCl, and 2.079 mmol of Bpy were mixed with 52.0 mmol of M, 17.3 mmol of B, and 2 mL

of benzonitrile. For a reaction time of 6060 s, the total monomer conversion was 60%. Copolymer characterization: butyl acrylate copolymer composition was 0.244, number-average molecular weight was 6700, and molecular weight distribution was 1.29.

Polymer Characterization. ^1H NMR spectroscopy was used to determine copolymer compositions. Spectra were recorded at 50 °C on about 8% solutions in deuteriochloroform using a Varian Oxford 300 spectrometer operating at 300 MHz. Typical parameters for the proton spectra were 9 μs , width 45°, pulse delay 0 s, adquisition time 3 s, 400 Hz spectral width, and 256 scans.

Sequence distribution and stereoregularity of the copolymers were studied by ^1H NMR and ^{13}C NMR, recorded at 50 °C with the same spectrometer. The parameters for the carbon spectra were the flip angle of 90° (pulse width 13 μs), delay time 3 s, 16 000 Hz spectral width, and acquisition time 1 s. A good signal-to-noise ratio was obtained using 15 000–30 000 scans. These conditions assured complete relaxation of all of the ^{13}C nuclei analyzed. Decoupling was gated on only during the acquisition to suppress any nuclear Overhauser enhancement. The signal intensities of the spectra peaks were measured from the integrated peak areas calculated with an electronic integrator.

Results and Discussion

Two different series of methyl methacrylate–butyl acrylate (M–B) copolymerization reactions were made. In bulk copolymerization although variation of $\ln [M]_0/[M]$ increased linearly with time, the experimental number-average molecular weights, M_n , were much higher than those theoretically predicted. The copolymer polydispersities were high, $1.3 < M_w/M_n < 1.7$, independent of conversion.

In the copolymerization performed in 25% (v/v) benzonitrile solution with the exchange halide technique, the variation of $\ln [M]_0/[M]$ increased linearly with time. They produced a good control in molecular weight, having very similar values to those predicted ones. Moreover, the polydispersities were lower, $M_w/M_n \leq 1.5$.

These two systems produce different molecular weights and molecular weight distributions due to the different solvent and initiator systems. These differences may affect intermolecular and intramolecular structures. Therefore, this paper will investigate the correlation of composition and microstructure with polymerization control.

The Mayo–Lewis terminal model¹⁰ is the simplest possible copolymerization model capable of explaining the experimental data. This model predicts the copolymer composition for a given monomer feed on the basis of just two parameters: the reactivity ratios r_M and r_B of monomers M and B, respectively. Most of the methods used to determinate monomer reactivity ratios are based on the composition differential equation. One of the most reliable methods is the Kelen–Tüdös¹¹ method.

The copolymer compositions were determined by ^1H NMR from the relative areas of the proton resonances of $-\text{OCH}_3$ ($\delta \approx 3.50$ – 3.65 ppm) of the M unit and $-\text{OCH}_2-$ ($\delta \approx 3.80$ – 4.00 ppm) of the B unit (Figure 1). The monomer reactivity ratios were obtained from the compositions of copolymers with conversions less than 50% using the modified equation¹² of Kelen–Tüdös. For the bulk copolymerization, $r_M = 1.49 \pm 0.14$ and $r_B = 0.46 \pm 0.05$. The values were similar for benzonitrile solution system ($r_M = 1.44 \pm 0.11$, $r_B = 0.56 \pm 0.06$).

The differences in these monomer reactivity ratios and those reported in the literature for this system^{5,7–9} may be due not only to different copolymerization

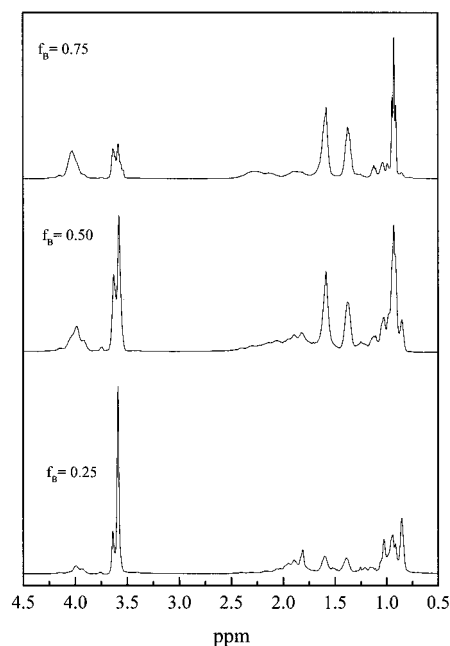


Figure 1. ^1H NMR spectra of M–B copolymers prepared by ATRP.

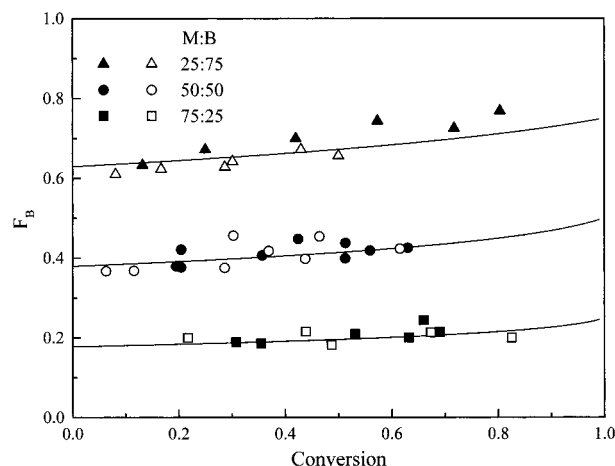


Figure 2. Cumulative copolymer composition of butyl acrylate, F_B , as a function of conversion. The solid lines have been calculated from the terminal model integrated copolymer equation with average monomer reactivity ratios determined. Open and solid symbols represent copolymer compositions obtained in bulk and benzonitrile solution, respectively.

temperatures¹³ and initiator/catalyst systems but also to the molecular weight variance.^{14,15}

Figure 2 shows the cumulative copolymer composition for both systems as a function of conversion for three feed compositions. The effect of conversion on the cumulative copolymer composition was approximated by a step function.¹⁶ The amount of each monomer polymerized is derived from the copolymerization theory. Then, the instantaneous copolymer composition for each step of the reaction is accumulated over the conversion to provide the integrated values. The solid lines were drawn according to this procedure using the Mayo–Lewis terminal model and the average of the monomer reactivity ratios from the bulk and benzonitrile systems. The experimental data are consistent with these reactivity ratios and the terminal model. The good agreement between theoretical and experimental cumulative copolymer composition seems to indicate that the active species formed in ATRP have similar chemoselectivity

to carbon-centered free radicals generated in a conventional free radical copolymerization.

As mentioned above, the sequence distribution is useful for investigating the polymerization mechanism, since it can discriminate between copolymerization models much better than composition.^{17,18} Most quantitative measurements in conventional free radical copolymerization were reported at low conversions; only a few studies were made at moderate or high conversions. To our knowledge, only qualitative results have been reported for ATRP copolymerizations. Therefore, this work carefully analyzes the sequence distribution and stereoregularity of copolymers prepared by ATRP by ¹H and ¹³C NMR spectra, not only to test the Mayo–Lewis terminal model but also to determine whether the copolymer microstructure and its variation with monomer conversion in living/controlled free radical polymerizations can be described by the same parameters as in conventional radical polymerizations.

The probability of each tactic sequence distribution formation is a function of monomer reactivity ratios and the monomer feed molar fraction. Because the monomer reactivity ratios values do not equal one, the monomer feed composition varies with conversion. Therefore, the monomeric sequence distribution along the main chain changes during the copolymerization. To correlate the molar concentration of M- and B-centered sequences with the stereochemical configuration of copolymer chains, our copolymer systems were analyzed statistically according to the monomer reactivity ratios; the conditional probabilities were calculated from the quoted reactivity ratios and monomer fraction in the feed. We made the following assumptions: (a) The chemical composition of copolymer sequence is described by Mayo–Lewis terminal model. (b) The configurational sequence distribution may be described according to Bernoullian statistics with the corresponding isotacticity and coisotacticity parameters, σ_M , σ_B , and $\sigma_{MB} = \sigma_{BM} = \sigma$.

Bovey and Coleman^{19,20} defined σ_i as the probability of generating a meso dyad between an i ending growing radical and an incoming j monomer. The isotacticity parameter for methyl methacrylate homopolymer was determined from the α -methyl resonance signal in the ¹H NMR spectrum by integrating the intensities of the signals at 1.19, 1.00, and 0.83 ppm, assigned to iso, hetero, and syndiotactic triads,²¹ respectively, giving a value of $\sigma_M = 0.23$.

The coisotacticity parameter was estimated following the assignment made by Brosse et al.²² for M–B conventional copolymerization for the methoxy (eqs 1 and 2).

$$\delta_{3.65 \text{ ppm}} = (1 - \sigma)^2 \text{BMB} + (1 - \sigma_M)(1 - \sigma) \text{MMB} \quad (1)$$

$$\delta_{3.60 \text{ ppm}} = \text{MMM} + [\sigma_M \sigma + \sigma_M(1 - \sigma) + (1 - \sigma_M)\sigma] \text{MMB} + [\sigma \sigma + 2\sigma(1 - \sigma)] \text{BMB} \quad (2)$$

Figure 1 shows the 300 MHz ¹H NMR spectra of different M–B copolymers. The methoxy resonance of the M-centered triads at 3.60 ppm is split. The relative intensities of the peaks at 3.60 and 3.65 ppm were compared with those calculated theoretically from eqs 1 and 2. The conditional probabilities of different triads involved in the previous equations were calculated at a determined conversion from the step function program using the monomer feed composition and the quoted

Table 1. Experimental Values of the Relative Intensities of the Methoxy of ¹H NMR Signal and Theoretical Values Calculated Using Brosse²² Assignments for Various Copolymers Prepared by ATRP at Different Monomer Feed Composition

f_B	F_B	conv (%)	experimental		theoretical	
			$\delta_{3.60 \text{ ppm}}$	$\delta_{3.65 \text{ ppm}}$	$\delta_{3.60 \text{ ppm}}$	$\delta_{3.65 \text{ ppm}}$
0.25	0.200	21.73	0.797	0.203	0.787	0.213
0.25	0.216	43.87	0.787	0.213	0.782	0.218
0.50	0.368	11.57	0.616	0.384	0.628	0.372
0.50	0.375	28.65	0.625	0.375	0.623	0.377
0.75	0.623	16.71	0.530	0.470	0.531	0.469
0.75	0.642	30.12	0.522	0.478	0.529	0.471

monomer reactivity ratios. The value of σ was determined by trial and error from these calculated values and σ_M . The resulting value of $\sigma = 0.30$ agrees with literature values for conventional radical copolymerizations.^{22,23} This indicates that random copolymers obtained by ATRP have the same tacticity as those prepared by classical radical procedures. Table 1 summarizes the molar feed composition, f_B , the molar copolymer composition, F_B , the experimentally observed peak areas, and the theoretically calculated areas. The excellent agreement between calculated and experimental data supports the ¹H NMR assignments.

The complex pattern of carbonyl ¹³C NMR resonance was analyzed to test the statistical and mechanism model considered. In addition, the relative stereochemical configuration of methyl methacrylate and butyl acrylate centered triads was considered for a complete description of the monomer sequence distributions. Figure 3 shows the carbonyl carbon resonances for the three copolymer compositions. There are seven distinguishable signals (I–VII) which change drastically with copolymer composition.

These signals were assigned to M- and B-centered triads according to the method reported by Aerdt et al.²³ Peaks I, II, IV, and VI correspond to different

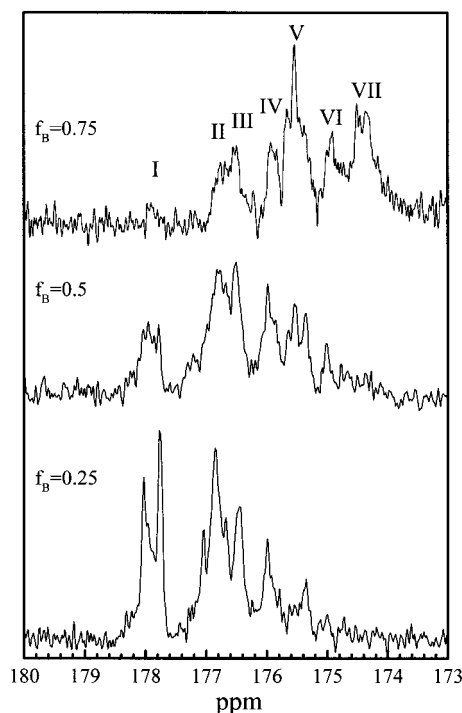


Figure 3. Expanded ¹³C NMR spectra showing the carbonyl region of M–B copolymers prepared by ATRP at different feed compositions.

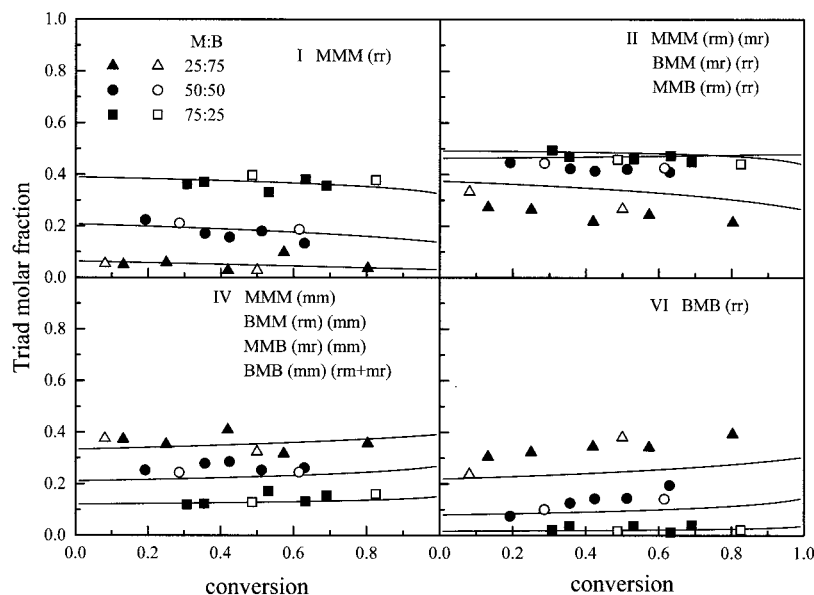


Figure 4. Relative intensity dependence of the carbonyl carbon peak areas of M-centered sequences as a function of total conversion. Open and solid symbols represent experimental data of bulk and benzonitrile solution, respectively. The solid lines are based and drawn on calculations made using $\sigma_M = 0.23$, $\sigma = 0.30$, $r_M = 1.49 \pm 0.14$, and $r_B = 0.46 \pm 0.05$.

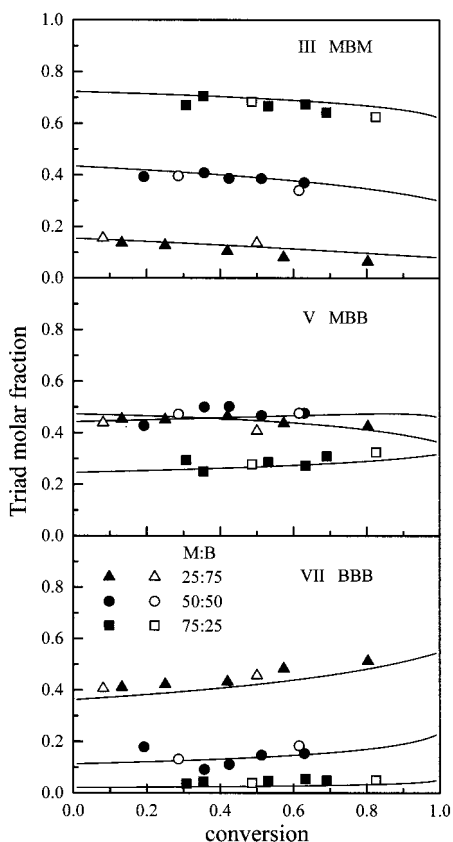


Figure 5. Relative intensity dependence of the carbonyl carbon peak areas of B-centered sequences as a function of total conversion. Open and solid symbols represent experimental data of bulk and benzonitrile solution, respectively. The solid lines are based and drawn on calculations made using $r_M = 1.49 \pm 0.14$ and $r_B = 0.46 \pm 0.05$.

configurational arrangements of M-centered triads. Peak I was assigned to MMM (rr) triads; peak II to MMM (rm + rm), BMM (mr + rr) and MMB (rm + rr); peak IV to MMM (mm), BMM (rm + mm), MMB (mr + mm) and BMB (mm + rm + mr); and peak VI to the BMB (rr) triad. Peaks III, V, and VII correspond to the

sequences and configurations of B-centered triads. These peaks were not sensitive to configuration of triad sequences. Peak III corresponds to MBM triad, peak V to MBB triad, and peak VII to BBB triad.

Comparison between theoretical and experimental values is represented in Figures 4 (for the spectral signal I, II, IV, and VI, methyl methacrylate centered triads) and 5 (for the regions III, V, and VII, according to B-centered triads) as a function of total monomer conversion. These figures present data for copolymer samples obtained both in bulk and benzonitrile solution at each of the three compositions studied over all range of conversions. Although there are slight deviations, the experimental and predicted values agree very closely. Despite the great difference in the control of molecular weight between both initiator/catalyst systems, all these copolymers have the same microstructure.

These results confirm the validity of the statistical parameters determined in this work, according to the Mayo–Lewis terminal model of copolymerization and Bernoullian stereochemical statistics of monomer units along the macromolecular chain. Therefore, the composition, sequence distribution, and stereoregularity of the copolymers are independent of the initiator/catalyst/solvent system used in our experimental conditions and are, therefore, independent of the level of control achieved in the polymerization. In addition, the inter- and intramolecular structure of copolymers synthesized by ATRP is the same as that of copolymers obtained by conventional radical polymerization.

Acknowledgment. This research was supported by the Comisión Interministerial de Ciencia y Tecnología (CICYT) (MAT97-682). Dr. M. Fernández-García is grateful to the Comunidad Autónoma de Madrid for financial support.

References and Notes

- (1) Koenig, J. L. In *Chemical Microstructure of Polymer Chains*; Wiley-Interscience: New York, 1980.
- (2) Tonelli, A. E. In *NMR Spectroscopy and Polymer Microstructure: The Conformational Connection*; VCH: New York, 1989.

- (3) (a) Georges, M. K.; Veregin, R. P. N.; Kazmaier, P. M.; Hamer, G. K.; *Trends Polym. Sci.* **1994**, 2, 66. (b) Davis, T. P.; Kukulj, D.; Haddleton, D. M.; Maloney, D. R. *Trends Polym. Sci.* **1995**, 3, 365. (c) Hawker, C. J.; *Trends Polym. Sci.* **1996**, 4, 371. (d) Sawamoto, M.; Kamigaito, M. *Trends Polym. Sci.* **1996**, 4, 371. (e) Matyjaszewski, K. Controlled Radical Polymerization. *ACS Symp. Ser.* **1998**, 685.
- (4) (a) Matyjaszewski, K. *J. Macromol. Sci., Pure Appl. Chem.* **1997**, A34, 1785. (b) Sawamoto, M.; Kamigaito, M. *J. Macromol. Sci., Pure Appl. Chem.* **1997**, A34, 1803. (c) Patten, T. E.; Matyjaszewski, K. *Adv. Mater.* **1998**, 10, 901. (d) Patten, T. E.; Matyjaszewski, K. *Acc. Chem. Res.* **1999**, 32, 898. (e) Matyjaszewski, K. *Chem. Eur. J.* **1999**, 5, 3095.
- (5) Moineau, G.; Minet, M.; Dubois, Ph.; Teyssié, Ph.; Senninger, T.; Jérôme, R. *Macromolecules* **1999**, 32, 27.
- (6) Uegaki, H.; Kotani, Y.; Kamigaito, M.; Sawamoto, M. *Macromolecules* **1998**, 31, 6756.
- (7) Roos, S. G.; Müller, A. H. E.; Matyjaszewski, K. *Macromolecules* **1999**, 32, 8331.
- (8) Arehart, S. V.; Matyjaszewski, K. *Polym. Prepr.* **1999**, 40, 458.
- (9) Ziegler, M. J.; Matyjaszewski, K. *Macromolecules*, **2001**, 34, 415.
- (10) Mayo, F. R.; Lewis, F. M. *J. Am. Chem. Soc.* **1944**, 66, 1594.
- (11) Tüdös, F.; Kelen, T.; Földes-Bereznich, T.; Turcsányi, B. *J. Macromol. Sci., Macromol. Chem.* **1976**, A10, 1513.
- (12) Kelen, T.; Tüdös, F.; Turcsányi, B.; Kennedy, J. P. *J. Polym. Sci., Polym. Chem. Ed.* **1977**, 15, 3047.
- (13) O'Driscoll, K. F. *J. Macromol. Sci., Chem.* **1969**, A3, 307.
- (14) Semchikov, YuD.; Smirnova, L. A.; Knyazewa, T. Ye.; Bulgakova, S. A.; Sherstyanykh, V. I. *Eur. Polym. J.* **1990**, 26, 883.
- (15) Semchikov, YuD. *Macromol. Symp.* **1996**, 111, 317.
- (16) Madruga, E. L.; Fernández-García, M. *Eur. Polym. J.* **1995**, 31, 1103.
- (17) Berger, M.; Kunz, I. *J. Polym. Sci.* **1964**, A2G, 1687.
- (18) Hill, D. J. T.; O'Donnell, J. H. *Makromol. Chem., Macromol. Symp.* **1987**, 10/11, 375.
- (19) Bovey, F. A. *J. Polym. Sci.* **1962**, 62, 197.
- (20) Coleman, B. *J. Polym. Sci.* **1958**, 31, 155.
- (21) Cuervo-Rodríguez, R.; Fernández-Monreal, M. C.; Fernández-García, M.; Madruga, E. L. *J. Polym. Sci., Polym. Chem.* **1997**, 35, 3483.
- (22) Brosse, J. C.; Gauthier, J. M.; Lenain, J. C. *Makromol. Chem.* **1983**, 184, 1379.
- (23) Aerdt, A. M.; German, A. L.; van der Velden, G. P. M. *Magn. Reson. Chem.* **1994**, 32, S80.

MA010428Y